HHS Public Access

Author manuscript

Addict Neurosci. Author manuscript; available in PMC 2023 September 01.

Published in final edited form as:

Addict Neurosci. 2023 September ; 7: . doi:10.1016/j.addicn.2023.100105.

Acute alcohol induces greater dose-dependent increase in the lateral cortical network functional connectivity in adult than adolescent rats

Sung-Ho Lee[a,b,c,d], **Tatiana A. Shnitko**[a,b,c], **Li-Ming Hsu**[a,b,c], **Margaret A. Broadwater**[a,b,c,d], **Mabelle Sardinas**[a,b,c], **Tzu-Wen Winnie Wang**[a,b,c], **Donita L. Robinson**[d,e], **Ryan P. Vetreno**[d,e], **Fulton T. Crews**[d,e,f], **Yen-Yu Ian Shih**[a,b,c,d,*]

[a]Center for Animal MRI, University of North Carolina, Chapel Hill, NC, USA

[b]Biomedical Research Imaging Center, University of North Carolina, Chapel Hill, NC, USA

[c]Department of Neurology, University of North Carolina, Chapel Hill, NC, USA

[d]Bowles Center for Alcohol Studies University of North Carolina, Chapel Hill, NC, USA

[e]Department of Psychiatry, University of North Carolina, Chapel Hill, NC, USA

[f]Department of Pharmacology, University of North Carolina, Chapel Hill, NC, USA

Abstract

Alcohol misuse and, particularly adolescent drinking, is a major public health concern. While evidence suggests that adolescent alcohol use affects frontal brain regions that are important for cognitive control over behavior little is known about how acute alcohol exposure alters large-scale brain networks and how sex and age may moderate such effects. Here, we employ a recently developed functional magnetic resonance imaging (fMRI) protocol to acquire rat brain functional connectivity data and use an established analytical pipeline to examine the effect of sex, age, and alcohol dose on connectivity within and between three major rodent brain networks: defaul mode, salience, and lateral cortical network. We identify the intra- and inter-network connectivity differences and establish moderation models to reveal significant influences of age on acute alcohol-induced lateral cortical network connectivity. Through this work, we make brain-wide isotropic fMRI data with acute alcohol challenge publicly available, with the hope to facilitate future discovery of brain regions/circuits that are causally relevant to the impact of acute alcohol use.

*Corresponding author at: Center for Animal MRI, University of North Carolina, 125 Mason Farm Road, CB# 7513, Chapel Hill, NC 27599, USA shihy@unc.edu (Y.-Y.I. Shih).

Declaration of Competing Interest

The authors declare that they have no known competing financial interests or personal relationships that could have appeared to influence the work reported in this paper.

CRediT authorship contribution statement

Sung-Ho Lee: Investigation, Writing – original draft. **Tatiana A. Shnitko:** Writing – original draft, Writing – review & editing. **Li-Ming Hsu:** Investigation. **Margaret A. Broadwater:** Conceptualization. **Mabelle Sardinas:** Investigation. **Tzu-Wen Winnie Wang:** Investigation. **Donita L. Robinson:** Conceptualization. **Ryan P. Vetreno:** Writing – review & editing. **Fulton T. Crews:** Conceptualization. **Yen-Yu Ian Shih:** Conceptualization, Writing – review & editing.

Keywords

Resting state fMRI; Connectivity; Rat; Underage drinking; Sex; Age

1. Introduction

Alcohol abuse is a significant public health concern and one of the leading causes of premature death and disability [1]. Despite legal constraints, adolescents (age 12–17) consume alcohol at alarming rate [2]. Early age of first alcohol intoxication is a critical risk factor for the development of alcohol use disorder [3–5]. One of the explanations concerning why early intoxication increases the risk of later alcohol problems is its interference with neurodevelopmental, hormonal and cognitive changes occurring at this age [6]. The frontal cortex undergoes substantial reorganization through adolescence [7–9], coinciding with ongoing puberty, improvement of executive functioning and top-down inhibitory control over behavior [10–12]. Several human imaging studies have suggested the frontal cortex may be particularly sensitive to alcohol [9,13–15]. Studies using rodent models have likewise found that adolescent frontal cortex is sensitive to the effects of chronic alcohol as reflected in persistent neuronal [16–18] and cognitive deficits [19,20]. Several recent brain imaging studies in rodents reported that adolescent alcohol exposure decreases cortical functional connectivity (FC) [21,22], glucose metabolism [23] and brain growth trajectories in rats [24]. Together, these studies suggest alterations in frontal cortical function after alcohol exposure during adolescence. However, it is relatively unknown how FC between the frontal cortex and other brain regions may be impacted by acute alcohol intoxication and whether sex and age are significant factors contributing to alcohol-induced FC changes. Gaining such knowledge using an experimental rodent model is important as it allows precise control of extraneous factors that are otherwise difficult to control in humans. The use of fMRI is also expected to facilitate translation of findings to humans.

The use of rodent models enables circuit, cellular, and molecular dissection of mechanisms related to alcohol use disorders and could shape our understanding about addiction development in the human brain. However, the evolutionary distinction of rodent frontal brain regions represents a gap between rodent and human findings. In humans, the frontal cortical regions exhibit a clear spatial segregation with different sub-regions linked to distinct large scale brain networks [25,26]. This spatial segregation is not as clear in rodents, as some network labels often show spatial overlaps in the rodent frontal cortex [27–29]. This cautions against considering only a single circuit/pathway in complex behaviors that have been associated with multiple large-scale networks, such as addiction [30,31]. Considering the urgent need to better understand rodent brain network systems, several pioneering efforts have been made to improve imaging protocols and share databases [32,33]. Joining these efforts, we recently developed a rat fMRI protocol at 400 mm isotropic spatial resolution and utilized data-driven parcellation with modularity analysis to obtain the “triple-network” features [27] that are homologues to human brain [25,26]. The triple-network model is widely adapted to characterize human brain function and dysfunction [34–36], including addiction [37–39]. Accumulating literature supports the existence of triple-networks in the rodent brain, including the salience network (SN) [40], default mode network (DMN) [41–

43] and lateral cortical network (LCN) [28,42,44]. Our recent Euclidean-based hierarchical clustering and Louvain modularity-based partitioning of the rat brain fMRI data further suggest that some frontal cortical regions may engage more than a single network [27] Collectively, these results indicate that in rodent brain (1) medial pre-frontal, cingulate, and retrosplenial cortices are nodes of the DMN, (2) sensorimotor cortices are nodes of the LCN, and (3) the medial pre-frontal, cingulate, anterior insular cortices, striatum, and amygdala and are nodes of the SN [27, 28]. While many of these nodes are currently the go-to targets in addiction research, the impact of alcohol on these nodes has yet to be examined at the network level. Consequently, that a brain-wide dynamic measure is required to understand the influence of alcohol on large-scale brain networks, and knowledge related to intra- and inter-network FC changes could pave the way toward a better understanding of alcohol addiction at a system level. Here, we report findings from an fMRI dataset studying the influence of age (PND45 and PND85), sex and acute dose-dependent effects of alcohol on intra- and inter-network connectivity of the triple-networks in rats.

2. Methods

2.1. Ethics statement

All experiments were in accordance with the Guide for the Care and Use of Laboratory Animals established by the National Institutes of Health, using protocols approved by the Institutional Animal Care and Use Committee at the University of North Carolina (UNC) at Chapel Hill.

2.2. Animals

A total of 38 Wistar rats bred and reared in-house were used in this experiment (breeders were purchased from Envigo in Dublin, VA). On postnatal day (P) 1, litters (n = 21) were culled to 8–10 pups, with the same ratio between sex whenever possible. The pups were housed with their mother until pair-housed at weaning (P21). The rats were divided into two groups composed of both sexes. Each group was then used for the resting-state fMRI (rs-fMRI) at age P45 (n = 19, 11 females) or P80 (n = 19, 10 females). Of note, the age effect was evaluated between independent groups to prevent the impact of prior exposure to the anesthetic at a later scan session. All animals were housed in a temperature- and humidity-controlled vivarium on a 12:12 h light:dark cycle with *ad libitum* access to food and water.

2.3. Experimental design

Each animal underwent a single scanning session at the designated age (P45 or P80). A total of 75 min of blood oxygenation level-dependent (BOLD) rs-fMRI data (five 15 min blocks) were acquired per single session. During the rs-fMRI scan session, each animal was given a saline i.p. injection after 15 min of the initial scan (baseline), followed by two 1 g/kg and one 2 g/kg of 20% v/v ethanol injections (one injection for each 15 min period) [45,46]. A timeline of ethanol dosing is represented in Fig. 4A. The volume of injected saline was determined based on the volume of the first ethanol injection. Consequently, the injection paradigm occurred with cumulative ethanol dose exposure for each injection session of 0, 1, 2, and 4 g/kg, respectively. The ethanol dosing protocol has been used in our

previous study where measures of blood ethanol concentration (BEC) were collected 15 min after the last dose [46]. The analysis revealed that cumulative 4 g/kg injected over 45 min interval resulted to average BEC of 96 ± 21 mg/dl (BEC range: 70–135 mg/dl). Imaging data from the baseline period (i.e., before alcohol administration including period after saline administration) were used to access the reproducibility of the rs-fMRI measures and effect of sex and age on triple-network FC in alcohol-naive rats.

2.4. MRI data acquisition

Rats were initially anesthetized with 4% isoflurane (Vaporizer #911103, VetEquip Inc., Livermore, CA, USA) mixed with medical air and endotracheally intubated using a 14G × 2"(P45) or 16G × 2"(P45) intravenous (i.v.) catheter (Surflash Polyurethane Catheter, TERUMO, Somerset, NJ, USA). Respiration was maintained by an MRI-compatible ventilator (MRI-1, CWE Inc, Ardmore, PA, USA) set at 60 breaths/min and an inspiration time ratio of 40%. Next, the isoflurane concentration was adjusted to 2% and the animals were secured to a custom-built, MR-compatible rat cradle. A rectal probe was used to monitor core body temperature (OAKTON Temp9500, Cole-Parmer, Vernon Hills, IL, USA) and a capnometer was used to monitor heart rate, peripheral blood oxygen saturation, and end-tidal CO_2 (SURGIVET® V90041LF, Smith Medical, Dublin, OH, USA). Body temperature was maintained at 37 ± 0.5 °C using a circulating water blanket connected to a temperature adjustable water bath (Haake S13, Thermo Fisher Scientific, Waltham, MA, USA). Ventilation tidal volume was adjusted to keep the heart rate at 300 ± 50 beats per minute, peripheral blood oxygen saturation above 96%, and end-tidal CO_2 between 2.8 and 3.2%. End-tidal CO_2 values from this capnometer system were previously calibrated against an invasive sampling of arterial blood gas, reflecting a partial pressure of carbon dioxide (pCO_2) level of 30–40 mm Hg [47,48]. Upon stabilizing the animals, a cocktail of dexmedetomidine (0.05 mg/kg/hr) and pancuronium bromide (0.5 mg/kg/hr) was continuously infused via the intraperitoneal cavity (i.p.) [21,49,50] and the isoflurane was reduced to 0.5% [51]. The infusion started 30 min prior to the rs-fMRI scans [41].

All MR images were collected through the UNC Center for Animal MRI (CAMRI) service on a Bruker BioSpec 9.4-Tesla, 30 cm bore system (Bruker BioSpin Corp., Billerica, MA) with ParaVision 6.0.1 on an AVANCE II console and an RRI BFG 240/120 gradient insert (up to 1000 mT/m gradient strength; Resonance Research, Inc, Billerica, MA) paired with a Prodrive BNG-500/1000 gradient amplifier (up to 500 A and 1000 V; Resonance Research, Inc, Billerica, MA). All experiments used an 86 mm volume coil as the RF transmitter (Bruker BioSpin Corp., Billerica, MA) and a 4-channel, rat brain array coil as the receiver (Bruker BioSpin Corp., Billerica, MA). Magnetic field homogeneity was first optimized by global shimming, followed by local second-order shims using a MAPSHIM protocol.

The BOLD rs-fMRI data were acquired using a 2D multi-slice, single-shot, gradient-echo EPI sequence: repetition time (TR) = 2000 ms, echo time (TE) = 14 ms bandwidth = 250 kHz, flip angle = 70°, field of view (FOV) = 28.8 × 28.8 mm, matrix size = 72 × 72, slice number = 32, and slice thickness = 0.4 mm, resulting in an isotropic voxel resolution of 0.4 mm.

2.5. Data analysis

2.5.1. MRI data preprocessing—All rs-fMRI data were first corrected for slice timing, followed by motion correction using AFNI [52]. Each 4D dataset was then averaged across time to improve signal-to-noise ratios (SNR) for subsequent skull stripping. The brain mask for each time-averaged EPI image was estimated using an in-house developed 2D-UNET-based machine learning algorithm [53] and was generated after manual refinement using ITK-snap [54]. This mask was subsequently applied to the corresponding rs-fMRI data to remove non-brain components. The skull-stripped data were then spatially normalized to the in-house developed EPI template [27] using ANTs SyN diffeomorphic registration [55] before further group-level analysis. For nuisance signal removal, third-degree polynomial curves representing baseline trend and the six motion parameters estimated from motion correction were regressed out, after which a 0.01–0.1 Hz band-pass filter was applied. The global signal was not regressed as discussed in our recent study [25]. The filtered data were then smoothed with a gaussian kernel with a full width half maximum (FWHM) at 0.5 mm. Finally, the data was segmented into five blocks of 15 min scans to represent the brain state of each exposure period. The first 5 min of data of each block containing injection periods (e.g., dynamic state) were discarded. Therefore, only 10 min data points for each block (e.g., steady state) were used in this study.

2.5.2. Statistical analysis of functional connectivity—To generate the functional connectivity matrix, the data-driven functional rat brain atlas from our previous study [27] was utilized as a set of regions of interest (ROIs). Time-course data were averaged within the identified ROIs and extracted from each subject and were used to calculate a Pearson's correlation coefficient matrix. The Fisher transformation was applied to convert the coefficient matrix to Gaussian distributed Fishers' z score for the group statistics. The fractions of edges were calculated on the network-level to abstract the within and between network connectivity. The order of ROIs of the resultant matrix was then re-ordered to make it represent the topological structure of the brain network-level as was identified in our previous study [27].

To evaluate the effects of sex, age, alcohol exposure, and alcohol dose, we employed a non-parametric, permutation-based, factorial analysis of variance (ANOVA) using a general linear model (GLM) approach. A design matrix for GLM was generated to evaluate four main factors: sex, age, before/after alcohol condition (main effect of alcohol), and dose of alcohol (0, 1, 2, 4 g/kg). A parametric factorial ANOVA was performed to calculate F values for each independent variable. Subsequently, the null distribution was generated by randomizing assigned factors. A total of 5000 iterations were applied for all permutation-based testing in this study. To control the family-wise error rate, we employed the min P/max T procedure, which counts the maximal T value or minimal p-value among the values generated at each iteration to form the null distribution. The significance of the test was defined as where T values from the one-sample t-test surpassed those of the null distribution at a p-value < 0.05.

2.5.3. Moderation analysis—A moderation analysis model was constructed using generalized linear mixed-effects (LME) model in MATLAB to analyze effect of sex

and age on ethanol induced changes in FC (MathWorks, Inc., [56]). In our work, the LME model was used instead of the general linear regression model to estimate the correlation coefficient between two variables for its ability to handle longitudinal data [57]. In each LME model, subject effects were included as the characterization of the temporal correlation. We first identified significant relationships between EtOH doses and the identified FC changes. Then, using this moderation model, both the age and sex were selected as two moderators of the association between EtOH doses and the identified FC changes. In this context, full moderation occurs when the relationship between the independent variable and the dependent variable is no longer significant with the inclusion of a moderator variable [56]. The moderation effect of each moderator for each dose-brain relationship was evaluated in the interaction between independent and moderator variables.

3. Results

3.1. Reproducibility and specificity of rs-fMRI measures

To assess the reproducibility of the rs-fMRI measures, a rs-fMRI matrix was formed from the baseline data collected prior to the ethanol injections. We compared the derived rs-fMRI matrix against our previously disseminated 87-subject database and found highly significant spatial similarity between the two datasets (Fig. 1), suggesting reliable measures of FC in the current cohort. To benchmark FC specificity of the current dataset, we implemented methods to evaluate individual specificity metric as described previously [27,32,33]. In this study, a higher FC between matching bilateral primary somatosensory cortex (S1) and a lower FC between S1 and retrosplenial cortex (RSC) within the same subject was considered specific. Using the thresholds of $Z(r) > 0.297$ for S1-S1 and $Z(r) < 0.061$ for S1-RSC, we identified 92.1% specificity from this dataset (Fig. 1), which was superior to the 73.6% specificity found in our previously disseminated dataset [27].

3.2. Sex and age effects on triple-networks

The GLM analysis revealed a significant main effect of sex on FC ($p < 0.05$ after family-wise error correction), with significant pairs of brain regions (i.e., edges) identified in Fig. 2A. Sex-dependent group-level FC matrices were contrasted between male and female subjects (collapsed across age, baseline and ethanol dosing) and significant differences in connectivity between the groups are shown in the figure. Next, we compared FC within and between the triple-networks and found the male subjects exhibited significantly higher intra-network FC within LCN, DMN, and SN; and inter-network FC between DMN and two other networks (Fig. 2 B, $p < 0.05$).

Further, the GLM also yielded a significant main effect of age on FC ($p < 0.05$ after family-wise error correction), with significant pairs of brain regions (i.e., edges) identified in Fig. 3A. One simple t test was employed to compare age-dependent FC within and between the triple-networks and found the P80 subjects to have significantly higher intra-network FC within DMN; and inter-network FC between DMN and SN (Fig. 3 B, $p < 0.05$).

3.3. Alcohol effect on population-level rs-fMRI changes

After baseline and saline data were collected, cumulative doses of 1, 2, and 4 g/kg were given to all subjects as described in the methods (Fig. 4A). Four groups of subjects went through this dose-protocol: adolescent (P45) female subjects, adolescent male subjects, adult (P80) female subjects, and adult male subjects. The entire population showed a general alcohol dose-dependent increase in FC between brain regions (within-network connectivity) and between networks. The GLM analysis revealed significant effect of ethanol exposure where condition-level FC matrices (i.e., in Fig. 4A, pre-alcohol (the first two blocks) vs. post-ethanol (collapsed three post-alcohol blocks) were derived and compared (effect of exposure, $p < 0.01$). The model also yielded a significant main effect of ethanol dose on FC (effect of dose, $p < 0.05$, Fig. 4B), with significant pairs of brain regions (i.e., edges). A follow up comparison of FC within and between the triple-networks revealed that acute EtOH significantly increases intra-network FC within LCN; and inter-network between LCN and DMN, and between LCN and SN (Fig. 4C).

Next, to unravel the influences of sex and age on the observed EtOH dose-dependent LCN-related FC changes, we employed three moderation analysis models (Fig. 5A). In these models, we set EtOH doses as dependent variables, the observed LCN-related FC increases (from Fig. 4C) as independent variables, and sex and age as moderators. Path analysis demonstrated significantly direct relationships between EtOH doses and the identified FC increases: within LCN (direct effect = 0.124, $p < 0.001$), between LCN and DMN (direct effect = 0.116, $p < 0.\ 001$), and between LCN and SN (direct effect = 0.090, $p < 0.\ 001$). All direct relationships were significantly moderated by age (interaction effect: all $p < 0.05$), but not by sex (interaction effect: all n.s.). Specifically, age showed significant partial moderation effects in all three models while the direct relationship between EtOH doses and LCN-related FC changes were still significant with the moderator (WM: all $p < 0.05$). Fig. 5B illustrates the dose-dependent increase in LCN-related FC in adolescent (P45) and adult (P80) rats.

The results of linear regression analysis are in Table 1. The results of this analysis indicate that adolescent subjects have less increase in EtOH-induced LCN-related FC than adults.

4. Discussion

The effect of acute alcohol on functional connectivity of DMN, SN and LCN in rats was examined using an established rs-fMRI data acquisition and analysis pipeline. First, we confirmed the reproducibility of rs-fMRI features by comparing the current cohort of subjects with our previously disseminated database [27]. Next, we revealed sex- and age-dependent differences in intro- and inter-network connectivity in rodent brain. Then we identified alcohol-induced an increase in FC within the LCN and between this network and SN and DMN. The moderation analysis revealed a significant effect of age in agreement with previously reported impact of age on behavioral responses in rats to acute alcohol [6, 58]. Overall, this study supports the utility of the rs-fMRI protocol in studying acute alcohol effects on brain networks and provides a topological roadmap to probe the mechanisms underlying the adolescent insensitivity to acute effects of alcohol intoxication.

This study utilized a rs-fMRI protocol capable of providing whole-brain coverage at 0.4 mm isotropic spatial resolution. The isotropic data enabled the use of 3D non-linear registration [55,59] and offered identical resolution along all the axes when deriving motion parameters [25], which facilitated rs-fMRI preprocessing steps. Using the established analytical pipeline and ROI labels as described in [27], we extracted intrinsic triple networks including the LCN, DMN, and SN (Fig. 1, [28,32,60]) that replicates our previous findings using a different dataset [25]. The triple-networks in the human brain [25] have been used widely to characterize human brain function and dysfunction [25,34–36]. Our previous study [27] identified hippocampus and cingulate cortex to be the nodes of DMN and insular cortex, nucleus accumbens, and amygdala to be the nodes of SN in the rat brain. These regions are analogous in humans and also nodes of the DMN and SN in the human brain, respectively.

The LCN includes areas of motor and somatosensory cortices, traditionally included in the sensorimotor network associated with motor learning and perceptual functions [61,62]. In the mammalian neocortex, cortical areas are functionally linked with each other, integrating, transforming, and passing information along to other areas. Thus, executive control over behavior results from a complex integrative process combining higher-level sensory processing and sensorimotor integration supported by somatosensory and motor cortices [63] included in the LCN in this study. While the *a priori* defined network nodes were derived from data-driven analyzes and allowed identification of distinct intra- and inter-network FC features in the current study, the precise functional topology of the rodent resting state networks remains a contentious issue in the field warranting behavioral validations in the future [24,25,84].

Development of alcohol use disorder differs between sexes and depends on age-related vulnerability. Understanding sex- and age-related differences in resting state FC may provide insights into risk and protective factors. In this study, connectivity within and between triple-networks was explored in male and female rats. Specifically, males (collapsed across both age groups) exhibited greater synchronization within all three networks, as well as between DMN and SN, LCN (Fig. 2). Heterogeneous evidence of sex-dependent differences in FC was reported in human and nonhuman primates [64–66]. Greater connectivity within DMN was previously shown in women versus men [67,68]; however, stronger synchronization of sensorimotor nodes (e.g., LCN in this study) was observed in men and male non-human primates [65,67]. Lack of sex-dependent differences in intrinsic FC within the triple networks was reported in humans [66]. Inconsistencies between results in human studies and reported here could be due to several factors known to significantly impact FC including use of anesthesia for data acquisition [69], collapsing samples across two age-groups [70] and contribution of the brain size differences [71].

This study revealed greater level of FC within the DMN and between this network and SN in adult rats compared to adolescents (Fig. 3). This finding corresponds to the previously reported age-dependent increase in intra- [72,73] and inter-network DMN-related connectivity [73–75]. In line with previous observations of age-related network connectivity, our results indicate strengthened synchronization of BOLD activity between the nodes of DMN and SN in rats. The reduced level of synchrony in the activity in adolescents might be underlined by individual differences in ongoing neurodevelopmental

process within the DMN regions including synaptic pruning and myelination completed in adulthood [76–79]. It is important to mention that adolescence is relatively short in rodents (between PND 28–42, with late adolescence extending to PND 55 [80]) compared to primates. Neurodevelopmental changes occurring across this age window are dynamic and significantly differ among early, middle and late adolescent periods [58,81]. The age-dependent differences observed in this study are specific to middle adolescence and, presumably, impacted by the developmental processes specific to this age. Thus, caution should be taken when interpreting the findings from the present study as it may not be generalizable across the entire adolescent period.

The neurodevelopmental changes occurring during adolescence is a significant factor contributing to vulnerability for developing alcohol use disorder [58]. In this study, acute alcohol intoxication dose-dependently increased intra- and inter connectivity of LCN that contains somatosensory and primary motor regions of the cortex (Fig. 4). Region-specific effect of acute alcohol on brain functional connectivity has been reported in humans. In agreement with results reported here, acute alcohol enhanced intra- and inter-network FC of somatosensory cortex in human brain [82,83]. However, reduced FC was reported between the areas of the frontal cortex, including prefrontal and anterior cingulate cortices, in young adults after acute alcohol [84]. In our previous study we investigated chronic and acute alcohol effects on FC between cortico-striatal regions associated with alcohol misuse [21]. Specifically, chronic alcohol exposure during adolescence resulted in reduced FC in adulthood within frontal cortical regions and between frontal cortical regions and striatum. In the same study, acute alcohol in adulthood enhanced cortico-striatal FC in alcohol-naïve animals, but not in rats with a history of adolescent alcohol exposure. The current study provides novel insights on the impact of acute alcohol on connectivity of sensorimotor cortices in alcohol-naïve animals. Acute alcohol enhanced intrinsic FC between these cortical regions as well as intra-network connectivity. While overall alcohol-related results in this study correspond to the previous research, the moderation analysis revealed an age-dependent effect in alcohol impact (Fig. 5). Age-dependent sensitivity to social, physical and cognitive effects of alcohol was previously reported in rodents, with adolescents being less responsive to alcohol dosing compared to adults [81,85,86]. This study provides novel insight on a possible network mechanism underlying blunted behavioral response to alcohol among adolescents.

While the rs-fMRI measures allow for assessment of acute and chronic alcohol effects on brain function, the mechanism underlying alcohol-induced change in FC remains incompletely understood. Several studies showed that acute alcohol decreases neuronal firing in the somatosensory cortex [87, 88]. Our recent fiber photometry study also showed that acute alcohol decreases calcium-dependent GCaMP activity in the prefrontal neurons [89]. Depending on the concentration, alcohol potentiates or inhibits calcium-dependent vasoconstriction [90–92], which subsequently alters local cerebral blood flow leading to a change in the BOLD fMRI signal [93]. Intriguingly, some previous studies reported an increase in the cerebral blood flow and reduced glucose utilization [94–96] after acute and chronic alcohol. The alcohol-induced decoupling between glucose metabolism and cerebral blood flow can be due to a shift in energy substrate toward an increase in metabolism of acetate as energy source, reported in humans after acute and chronic alcohol [96]. Glucose is

essential for the synthesis of the glutamate-precursor glutamine [97], and alcohol misuse has been linked to a deficit in extracellular glutamate levels and an altered balance between the glutamate-dependent excitatory and GABA-dependent inhibitory neurotransmission systems [98,99]. Nevertheless, it should be noted that decrease in neuronal activity or glucose metabolism does not necessarily come with a decrease in FC (i.e., enhanced synchronization can occur at lower amplitude of activity), and involvement of vasoactive neurotransmission can lead to decoupling between neuronal activity and flow [60,100,101]. In a recent study, Ochi and colleagues (2022) reported an inverted correlation between alcohol-induced increase in cortical FC and somatostatin cortical gene expression in human brain, suggesting that alcohol-induced inhibition of GABAergic interneurons might underly the change in connectivity [83]. Indeed, the GABAergic system is closely related to alcohol-induced activity changes [102–104]. Inhibition of GABA interneurons would lead to presumably synchronized disinhibition of projecting pyramidal neurons, which might be reflected by increased connectivity between cortical brain regions. Importantly, developmental changes of GABA-mediated inhibition in the somatosensory and prefrontal cortices during adolescence have been also reported in rodents [105–107], suggesting a potential role of GABA-interneurons in age-dependent differences in alcohol effect on FC observed in this study. Future studies combining different recording modalities such as FSCV-fMRI [108], electrophysiology [109–111] and fiber photometry [112, 113] can help reveal the potential role of GABAergic interneurons in alcohol-induced increase in cortical FC.

This study has few limitations. The fcMRI data acquisition was conducted with continuous infusion of dexmedetomidine plus low-dose isoflurane. While this protocol is broadly utilized in rodents [114], isoflurane is known to act through the GABAergic mechanism in the brain [115, 116], and the combination with dexmedetomidine, an alpha-2 adrenergic agonist, might interact with alcohol to alter alcohol-induced FC changes. It is therefore important to note that the observed FC changes may differ in non-anaesthetized subjects. Specifically, the cognition- and perception-related network changes are expected to lessen in the current anaesthetized setting, while the pharmacological effects of alcohol may be accentuated. Future studies performing fMRI in awake rodents can address this caveat [117–121]. Additionally, this study uses the cumulative ethanol dosing via i.p. route. While this dosing approach mimics intoxication in humans during a drinking episode, it makes it difficult to identify the exact dose and timing effects on functional connectivity. Nevertheless, using proton magnetic resonance spectroscopy (MRS) in rats, Adalsteinsson and collogues (2006) have revealed a rapid increase (within 7 min) in brain ethanol concentration after 1 g/kg dose (i.p.) followed by its slow decay at the rate of −0.21 mg%/min; whereas Carton and collogues (2019) used MRS and gas chromatography analysis to reveal that cerebral and blood ethanol concentration peaks at 30 min post 1 and 2 g/kg dose [99]. These results suggest the variability in cerebral kinetics of ethanol kinetics in the brain, individual differences in the rate of ethanol absorption, first-pass effect associated with i.p. delivery, and ethanol decay in the brain within the 15 min epoch preceding the following injection may represent confounding factors of our study. Future studies with real-time BEC measurement are needed to reveal the exact dose-connectivity relationship beyond what is reported in this work.

Funding

This research was supported by the National Institutes of Health, NIAAA (U01AA020023, P60AA011605, K01AA025383), NIMH (R01MH126518, R01MH111429, RF1MH117053, S10MH124745), NINDS (R01NS091236), NICHD (P50HD103573), and Office of the Director (S10OD026796). We thank the members of the UNC Center for Animal MRI and Bowles Center for Alcohol Studies for their inputs.

Data availability

Data will be made available on request.

References

[1]. Sohi I, Franklin A, Chrystoja B, Wettlaufer A, Rehm J, Shield K, The global impact of alcohol consumption on premature mortality and health in 2016, Nutrients 13 (9) (2021), doi: 10.3390/nu13093145.

[2]. Miech RA, Johnston DL, Patrick ME, O'Malley PM, Bachman JG, Schulenberg JE, Monitoring the future national surveyresults on drug use, 1975–2022, Secondary SchoolStudents, Institute for Social Research, The University of Michigan, Ann Arbor, 2023.

[3]. DeWit DJ, Adlaf EM, Offord DR, Ogborne AC, Age at first alcohol use: a risk factor for the development of alcohol disorders, Am J Psychiatry 157 (5) (2000) 745–750, doi: 10.1176/appi.ajp.157.5.745. [PubMed: 10784467]

[4]. Henry KL, McDonald JN, Oetting ER, Walker PS, Walker RD, Beauvais F, Age of onset of first alcohol intoxication and subsequent alcohol use among urban American Indian adolescents, Psychol. Addict. Behav. 25 (1) (2011) 48–56, doi: 10.1037/a0021710. [PubMed: 21244122]

[5]. Morean ME, Kong G, Camenga DR, Cavallo DA, Connell C, Krishnan-Sarin S, First drink to first drunk: age of onset and delay to intoxication are associated with adolescent alcohol use and binge drinking, Alcohol Clin. Exp. Res. 38 (10) (2014) 2615–2621, doi: 10.1111/acer.12526. [PubMed: 25257574]

[6]. Spear LP, Adolescents and alcohol: acute sensitivities, enhanced intake, and later consequences, Neurotoxicol. Teratol. 41 (2014) 51–59, doi: 10.1016/j.ntt.2013.11.006. [PubMed: 24291291]

[7]. Perica MI, Calabro FJ, Larsen B, et al. , Development of frontal GABA and glutamate supports excitation/inhibition balance from adolescence into adulthood, Prog. Neurobiol. (2022) 102370 Published online October 26, doi: 10.1016/j.pneurobio.2022.102370.

[8]. Walker CD, Sexton HG, Hyde J, Greene B, Risher ML, Diverging effects of adolescent ethanol exposure on tripartite synaptic development across prefrontal cortex subregions, Cells 11 (19) (2022), doi: 10.3390/cells11193111.

[9]. Luo X, Yang JJ, Buu A, Trucco EM, R Li CS, Alcohol and cannabis co-use and longitudinal gray matter volumetric changes in early and late adolescence, Addict. Biol. 27 (5) (2022) e13208, doi: 10.1111/adb.13208.

[10]. Saito DN, Fujisawa TX, Yanaka HT, et al. , Development of attentional networks during childhood and adolescence: a functional MRI study, Neuropsychopharmacol. Rep. 42 (2) (2022) 191–198, doi: 10.1002/npr2.12246. [PubMed: 35266330]

[11]. Sung D, Park B, Kim B, et al. , Gray matter volume in the developing frontal lobe and its relationship with executive function in late childhood and adolescence: a community-based study, Front. Psychiatry 12 (2021) 686174, doi: 10.3389/fp-syt.2021.686174. [PubMed: 34326786]

[12]. Sisk CL, Development: pubertal hormones meet the adolescent brain, Curr. Biol. 27 (14) (2017) R706–R708, doi: 10.1016/j.cub.2017.05.092. [PubMed: 28743017]

[13]. Squeglia LM, Tapert SF, Sullivan EV, et al. , Brain development in heavy-drinking adolescents, Am. J. Psychiatry 172 (6) (2015) 531–542, doi: 10.1176/appi.ajp.2015.14101249. [PubMed: 25982660]

[14]. Bava S, Jacobus J, Thayer RE, Tapert SF, Longitudinal changes in white matter integrity among adolescent substance users, Alcohol Clin. Exp. Res. 37 (2013) E181–E189 Suppl 1, doi: 10.1111/j.1530-0277.2012.01920.x. [PubMed: 23240741]

[15]. Sun D, Adduru VR, Phillips RD, et al. , Adolescent alcohol use is linked to disruptions in age-appropriate cortical thinning: an unsupervised machine learning approach, Neuropsychopharmacology (2022) Published online October 8, doi: 10.1038/s41386-022-01457-4.

[16]. Crews FT, Braun CJ, Hoplight B, Switzer RC, Knapp DJ, Binge ethanol consumption causes differential brain damage in young adolescent rats compared with adult rats, Alcohol Clin. Exp. Res. 24 (11) (2000) 1712–1723. [PubMed: 11104119]

[17]. Vetreno RP, Yaxley R, Paniagua B, Johnson GA, Crews FT, Adult rat cortical thickness changes across age and following adolescent intermittent ethanol treatment, Addict. Biol. 22 (3) (2017) 712–723, doi: 10.1111/adb.12364. [PubMed: 26833865]

[18]. Dannenhoffer CA, Gómez-A A, Macht VA, et al. , Impact of adolescent intermittent ethanol exposure on interneurons and their surrounding perineuronal nets in adulthood, Alcohol Clin. Exp. Res. 46 (5) (2022) 759–769, doi: 10.1111/acer.14810. [PubMed: 35307830]

[19]. Gass JT, Trantham-Davidson H, Kassab AS, Glen WB, Olive MF, Chandler LJ, Enhancement of extinction learning attenuates ethanol-seeking behavior and alters plasticity in the prefrontal cortex, J. Neurosci. 34 (22) (2014) 7562–7574, doi: 10.1523/JNEUROSCI.5616-12.2014. [PubMed: 24872560]

[20]. Sey NYA, Gómez-A A, Madayag AC, Boettiger CA, Robinson DL, Adolescent intermittent ethanol impairs behavioral flexibility in a rat foraging task in adulthood, Behav. Brain Res. 373 (2019) 112085, doi: 10.1016/j.bbr.2019.112085.

[21]. Broadwater MA, Lee SH, Yu Y, et al. , Adolescent alcohol exposure decreases frontostriatal resting-state functional connectivity in adulthood, Addict. Biol. 23 (2) (2018) 810–823, doi: 10.1111/adb.12530. [PubMed: 28691248]

[22]. Gómez-A A, Dannenhoffer CA, Elton A, et al. , Altered cortico-subcortical network after adolescent alcohol exposure mediates behavioral deficits in flexible decision-making, Front. Pharmacol. 12 (2021) 778884, doi: 10.3389/fphar.2021.778884. [PubMed: 34912227]

[23]. Rapp C, Hamilton J, Richer K, Sajjad M, Yao R, Thanos PK, Alcohol binge drinking decreases brain glucose metabolism and functional connectivity in adolescent rats, Metab. Brain Dis. 37 (6) (2022) 1901–1908, doi: 10.1007/s11011-022-00977-8. [PubMed: 35567647]

[24]. Piekarski DJ, Zahr NM, Zhao Q, Sullivan EV, Pfefferbaum A Alcohol's effects on the mouse brain are modulated by age and sex, Addict. Biol. 27 (5) (2022) e13209, doi: 10.1111/adb.13209.

[25]. Menon V, Large-scale brain networks and psychopathology: a unifying triple network model, Trends Cogn. Sci. 15 (10) (2011) 483–506 (Regul Ed), doi: 10.1016/j.tics.2011.08.003. [PubMed: 21908230]

[26]. Menon VD, Esposito M, The role of PFC networks in cognitive control and executive function, Neuropsychopharmacology 47 (1) (2022) 90–103, doi: 10.1038/s41386-021-01152-w. [PubMed: 34408276]

[27]. H Lee S, Broadwater MA, Ban W, et al. , An isotropic EPI database and analytical pipelines for rat brain resting-state fMRI, NeuroImage 243 (2021) 118541, doi: 10.1016/j.neuroimage.2021.118541. [PubMed: 34478824]

[28]. Mandino F, Vrooman RM, Foo HE, et al. , A triple-network organization for the mouse brain, Mol. Psychiatry 27 (2) (2022) 865–872, doi: 10.1038/s41380-021-01298-5. [PubMed: 34650202]

[29]. Chao THH, Lee B, Hsu LM, et al. , Neuronal dynamics of the default mode network and anterior insular cortex: Intrinsic properties and modulation by salient stimuli, biorxiv (2022) Published online August 3, doi: 10.1101/2022.08.01.501899.

[30]. Zhang R, Volkow ND, Brain default-mode network dysfunction in addiction, NeuroImage 200 (2019) 313–331, doi: 10.1016/j.neuroimage.2019.06.036. [PubMed: 31229660]

[31]. Orsini CA, Colon-Perez LM, Heshmati SC, Setlow B, Febo M, Functional connectivity of chronic cocaine use reveals progressive neuroadaptations in neocortical, striatal, and limbic networks, eNeuro 5 (4) (2018), doi: 10.1523/ENEURO.0081-18.2018.

[32]. Grandjean J, Canella C, Anckaerts C, et al. , Common functional networks in the mouse brain revealed by multi-centre resting-state fMRI analysis, NeuroImage 205 (2020) 116278, doi: 10.1016/j.neuroimage.2019.116278. [PubMed: 31614221]

[33]. Liu Y, Q Fu H, Wu Y, et al. , Influence of three different anesthesia protocols on aged rat brain: a resting-state functional magnetic resonance imaging study, Chin. Med. J. 134 (3) (2020) 344–352, doi: 10.1097/CM9.0000000000001126. [PubMed: 33074843]

[34]. Bullmore E, Sporns O, Complex brain networks: graph theoretical analysis of structural and functional systems, Nat. Rev. Neurosci. 10 (3) (2009) 186–198, doi: 10.1038/nrn2575. [PubMed: 19190637]

[35]. Menon B, Towards a new model of understanding - the triple network, psychopathology and the structure of the mind, Med. Hypotheses 133 (2019) 109385, doi: 10.1016/j.mehy.2019.109385. [PubMed: 31494485]

[36]. Rubinov M, Sporns O, Complex network measures of brain connectivity: uses and interpretations, NeuroImage 52 (3) (2010) 1059–1069, doi: 10.1016/j.neuroimage.2009.10.003. [PubMed: 19819337]

[37]. Imperatori C, Massullo C, Carbone GA, et al. , Increased resting state triple network functional connectivity in undergraduate problematic cannabis users: A preliminary EEG coherence study, Brain Sci. 10 (3) (2020), doi: 10.3390/brain-sci10030136.

[38]. Zhang JT, Ma SS, Yan CG, et al. , Altered coupling of default-mode, executive-control and salience networks in Internet gaming disorder, Eur. Psychiatry 45 (2017) 114–120, doi: 10.1016/j.eurpsy.2017.06.012. [PubMed: 28756109]

[39]. Zhai T, Gu H, Salmeron BJ, Stein EA, Yang Y, Disrupted dynamic interactions between large-scale brain networks in cocaine users are associated with dependence severity, Biol. Psychiatry Cogn. Neurosci. Neuroimaging (2022) Published online September 2, doi: 10.1016/j.bpsc.2022.08.010.

[40]. Tsai PJ, Keeley RJ, Carmack SA, et al. , Converging structural and functional evidence for a rat salience network, Biol. Psychiatry 88 (11) (2020) 867–878, doi: 10.1016/j.biopsych.2020.06.023. [PubMed: 32981657]

[41]. Lu H, Zou Q, Gu H, Raichle ME, Stein EA, Yang Y, Rat brains also have a default mode network, Proc. Natl. Acad. Sci. U. S. A. 109 (10) (2012) 3979–3984, doi: 10.1073/pnas.1200506109. [PubMed: 22355129]

[42]. Gozzi A, Schwarz AJ, Large-scale functional connectivity networks in the rodent brain, NeuroImage 127 (2016) 496–509, doi: 10.1016/j.neuroimage.2015.12.017. [PubMed: 26706448]

[43]. Whitesell JD, Liska A, Coletta L, et al. , Regional, layer, and cell-type-specific connectivity of the mouse default mode network, Neuron 109 (3) (2021) 545–559 e8, doi: 10.1016/j.neuron.2020.11.011. [PubMed: 33290731]

[44]. Schwarz AJ, Gass N, Sartorius A, et al. , Anti-correlated cortical networks of intrinsic connectivity in the rat brain, Brain Connect. 3 (5) (2013) 503–511, doi: 10.1089/brain.2013.0168. [PubMed: 23919836]

[45]. Shnitko TA, Kennerly LC, Spear LP, DL. Robinson, Ethanol reduces evoked dopamine release and slows clearance in the rat medial prefrontal cortex, Alcohol Clin. Exp. Res. 38 (12) (2014) 2969–2977, doi: 10.1111/acer.12587. [PubMed: 25581652]

[46]. Shnitko TA, Spear LP, Robinson DL, Adolescent binge-like alcohol alters sensitivity to acute alcohol effects on dopamine release in the nucleus accumbens of adult rats, Psychopharmacology 233 (3) (2016) 361–371 (Berl), doi: 10.1007/s00213-015-4106-8. [PubMed: 26487039]

[47]. YI Shih Y, C Chiang Y, C Shyu B, Jaw FS, Duong TQ, Chang C, Endogenous opioid-dopamine neurotransmission underlie negative CBV fMRI signals, Exp. Neurol. 234 (2) (2012) 382–388, doi: 10.1016/j.expneurol.2011.12.042. [PubMed: 22245158]

[48]. YI Shih Y, Y Chen Y, Y Lai H, CJ Kao Y, C Shyu B, Duong TQ, Ultra high-resolution fMRI and electrophysiology of the rat primary somatosensory cortex, NeuroImage 73 (2013) 113–120, doi: 10.1016/j.neuroimage.2013.01.062. [PubMed: 23384528]

[49]. Albaugh DL, Salzwedel A, Van Den Berge N, Gao W, Stuber GD, YI Y. Shih, Functional magnetic resonance imaging of electrical and optogenetic deep brain stimulation at the rat nucleus accumbens, Sci. Rep. 6 (2016) 31613, doi: 10.1038/srep31613. [PubMed: 27601003]

[50]. Pawela CP, Biswal BB, Hudetz AG, et al. , A protocol for use of medetomidine anesthesia in rats for extended studies using task-induced BOLD contrast and resting-state functional

connectivity, NeuroImage 46 (4) (2009) 1137–1147, doi: 10.1016/j.neuroimage.2009.03.004. [PubMed: 19285560]

[51]. Fukuda M, Vazquez AL, Zong X, Kim SG, Effects of the α_2-adrenergic receptor agonist dexmedetomidine on neural, vascular and BOLD fMRI responses in the somatosensory cortex, Eur. J. Neurosci. 37 (1) (2013) 80–95, doi: 10.1111/ejn.12024. [PubMed: 23106361]

[52]. Cox RW, AFNI: software for analysis and visualization of functional magnetic resonance neuroimages, Comput. Biomed. Res. 29 (3) (1996) 162–173, doi: 10.1006/cbmr.1996.0014. [PubMed: 8812068]

[53]. M Hsu L, Wang S, Ranadive P, et al. , Automatic skull stripping of rat and mouse brain mri data using U-net, Front. Neurosci. 14 (2020) 568614, doi: 10.3389/fnins.2020.568614. [PubMed: 33117118]

[54]. Yushkevich PA, Piven J, Hazlett HC, et al. , User-guided 3D active contour segmentation of anatomical structures: significantly improved efficiency and reliability, NeuroImage 31 (3) (2006) 1116–1128, doi: 10.1016/j.neuroimage.2006.01.015. [PubMed: 16545965]

[55]. Avants BB, Epstein CL, Grossman M, Gee JC, Symmetric diffeomorphic image registration with cross-correlation: evaluating automated labeling of elderly and neurodegenerative brain, Med. Image Anal. 12 (1) (2008) 26–41, doi: 10.1016/j.media.2007.06.004. [PubMed: 17659998]

[56]. Baron RM, Kenny DA, The moderator–mediator variable distinction in social psychological research: conceptual, strategic, and statistical considerations, J. Pers. Soc. Psychol. 51 (6) (1986) 1173–1182, doi: 10.1037/0022-3514.51.6.1173. [PubMed: 3806354]

[57]. Avilés AI, Linear mixed models for longitudinal data, Technometrics 43 (3) (2001).

[58]. Spear LP, The adolescent brain and age-related behavioral manifestations, Neurosci. Biobehav. Rev. 24 (4) (2000) 417–463, doi: 10.1016/s0149-7634(00)00014-2. [PubMed: 10817843]

[59]. Avants BB, Tustison NJ, Song G, Cook PA, Klein A, Gee JC, A reproducible evaluation of ANTs similarity metric performance in brain image registration, NeuroImage 54 (3) (2011) 2033–2044, doi: 10.1016/j.neuroimage.2010.09.025. [PubMed: 20851191]

[60]. Oyarzabal EA, M Hsu L, Das M, et al. , Chemogenetic stimulation of tonic locus coeruleus activity strengthens the default mode network, Sci. Adv. 8 (17) (2022) eabm9898, doi: 10.1126/sciadv.abm9898.

[61]. Zhang J, Su J, Wang M, et al. , The sensorimotor network dysfunction in migraineurs without aura: a resting-state fMRI study, J. Neurol. 264 (4) (2017) 654–663, doi: 10.1007/s00415-017-8404-4. [PubMed: 28154971]

[62]. Vahdat S, Darainy M, Milner TE, DJ. Ostry, Functionally specific changes in resting-state sensorimotor networks after motor learning, J. Neurosci. 31 (47) (2011) 16907–16915, doi: 10.1523/JNEUROSCI.2737-11.2011. [PubMed: 22114261]

[63]. Ni J, Chen JL, Long-range cortical dynamics: a perspective from the mouse sensorimotor whisker system, Eur. J. Neurosci. 46 (8) (2017) 2315–2324, doi: 10.1111/ejn.13698. [PubMed: 28921729]

[64]. Filippi M, Valsasina P, Misci P, Falini A, Comi G, Rocca MA, The organization of intrinsic brain activity differs between genders: a resting-state fMRI study in a large cohort of young healthy subjects, Hum. Brain Mapp. 34 (6) (2013) 1330–1343, doi: 10.1002/hbm.21514. [PubMed: 22359372]

[65]. Nephew BC, Febo M, Cali R, et al. , Robustness of sex-differences in functional connectivity over time in middle-aged marmosets, Sci. Rep. 10 (1) (2020) 16647, doi: 10.1038/s41598-020-73811-9. [PubMed: 33024242]

[66]. Weissman-Fogel I, Moayedi M, Taylor KS, Pope G, Davis KD, Cognitive and default-mode resting state networks: do male and female brains “rest” differently? Hum. Brain Mapp. 31 (11) (2010) 1713–1726, doi: 10.1002/hbm.20968. [PubMed: 20725910]

[67]. Allen EA, Erhardt EB, Damaraju E, et al. , A baseline for the multivariate comparison of resting-state networks, Front. Syst. Neurosci. 5 (2011) 2, doi: 10.3389/fn-sys.2011.00002. [PubMed: 21442040]

[68]. Biswal BB, Mennes M, N Zuo X, et al. , Toward discovery science of human brain function, Proc. Natl. Acad. Sci. U. S. A. 107 (10) (2010) 4734–4739, doi: 10.1073/pnas.0911855107. [PubMed: 20176931]

[69]. Xie H, Chung DY, Kura S, et al. , Differential effects of anesthetics on resting state functional connectivity in the mouse, J. Cereb. Blood Flow Metab. 40 (4) (2020) 875–884, doi: 10.1177/0271678x19847123. [PubMed: 31092086]

[70]. Scheinost D, Finn ES, Tokoglu F, et al. , Sex differences in normal age trajectories of functional brain networks, Hum. Brain Mapp. 36 (4) (2015) 1524–1535, doi: 10.1002/hbm.22720. [PubMed: 25523617]

[71]. Li M, Wang J, Liu F, et al. , Handedness- and brain size-related efficiency differences in small-world brain networks: a resting-state functional magnetic resonance imaging study, Brain Connect. 5 (4) (2015) 259–265, doi: 10.1089/brain.2014.0291. [PubMed: 25535788]

[72]. Fair DA, Cohen AL, Dosenbach NUF, et al. , The maturing architecture of the brain's default network, Proc. Natl. Acad. Sci. U. S. A. 105 (10) (2008) 4028–4032, doi: 10.1073/pnas.0800376105. [PubMed: 18322013]

[73]. Pruitt PJ, Tang L, Hayes JM, Ofen N, JS. Damoiseaux, Lifespan differences in background functional connectivity of core cognitive large-scale brain networks, Neurosci. Res. 16 (2022) Published online September, doi: 10.1016/j.neures.2022.09.005.

[74]. Betzel RF, Byrge L, He Y, Goñi J, N Zuo X, Sporns O, Changes in structural and functional connectivity among resting-state networks across the human lifespan, NeuroImage (2014) 345–357 102 Pt 2, doi: 10.1016/j.neuroimage.2014.07.067.

[75]. Chen Y, Zhao X, Zhang X, et al. , Age-related early/late variations of functional connectivity across the human lifespan, Neuroradiology 60 (4) (2018) 403–412, doi: 10.1007/s00234-017-1973-1. [PubMed: 29383434]

[76]. Rakic P, P Bourgeois J, Goldman-Rakic PS, Synaptic development of the cerebral cortex: implications for learning, memory, and mental illness, in: The Self-Organizing Brain: From Growth Cones to Functional Networks, Elsevier, 1994, pp. 227–243, doi: 10.1016/S0079-6123(08)60543-9. Vol 102. Progress in brain research.

[77]. Huttenlocher PR, AS. Dabholkar, Regional differences in synaptogenesis in human cerebral cortex, J. Comput. Neurol. 387 (2) (1997) 167–178 doi: 10.1002/(sici)1096-9861(19971020)387:2<167::aid-cne1>3.0.co;2-z.

[78]. Markham JA, Greenough WT, Experience-driven brain plasticity: beyond the synapse, Neuron Glia Biol. 1 (4) (2004) 351–363, doi: 10.1017/s1740925x05000219. [PubMed: 16921405]

[79]. Gilmore JH, Knickmeyer RC, Gao W, Imaging structural and functional brain development in early childhood, Nat. Rev. Neurosci. 19 (3) (2018) 123–137, doi: 10.1038/nrn.2018.1. [PubMed: 29449712]

[80]. Robinson DL, Amodeo LR, Chandler LJ, et al. , The role of sex in the persistent effects of adolescent alcohol exposure on behavior and neurobiology in rodents, Int. Rev. Neurobiol. 160 (2021) 305–340, doi: 10.1016/bs.irn.2021.07.007. [PubMed: 34696877]

[81]. Spear LP, Adolescence VEI, Alcohol sensitivity, tolerance, and intake, Recent Dev. Alcohol. 17 (2005) 143–159. [PubMed: 15789864]

[82]. Han J, Keedy S, Murray CH, Foxley S, de Wit H, Acute effects of alcohol on resting-state functional connectivity in healthy young men, Addict. Behav. 115 (2021) 106786, doi: 10.1016/j.addbeh.2020.106786. [PubMed: 33421747]

[83]. Ochi R, Ueno F, Sakuma M, et al. , Patterns of functional connectivity alterations induced by alcohol reflect somatostatin interneuron expression in the human cerebral cortex, Sci. Rep. 12 (1) (2022) 7896, doi: 10.1038/s41598-022-12035-5. [PubMed: 35550587]

[84]. Sherman LE, Rosenbaum GM, Smith AR, et al. , The interactive effects of peers and alcohol on functional brain connectivity in young adults, NeuroImage 197 (2019) 264–272, doi: 10.1016/j.neuroimage.2019.04.003. [PubMed: 30978496]

[85]. Varlinskaya EI, LP. Spear, Acute effects of ethanol on social behavior of adolescent and adult rats: role of familiarity of the test situation, Alcohol Clin. Exp. Res. 26 (10) (2002) 1502–1511, doi: 10.1097/01.ALC.0000034033.95701.E3. [PubMed: 12394283]

[86]. Van Skike CE, Botta P, Chin VS, et al. , Behavioral effects of ethanol in cerebellum are age dependent: potential system and molecular mechanisms, Alcohol Clin. Exp. Res. 34 (12) (2010) 2070–2080, doi: 10.1111/j.1530-0277.2010.01303.x. [PubMed: 20860615]

[87]. Chapin JK, Sorensen SM, DJ. Woodward, Acute ethanol effects on sensory responses of single units in the somatosensory cortex of rats during different behavioral states, Pharmacol. Biochem. Behav. 25 (3) (1986) 607–614, doi: 10.1016/0091-3057(86)90149-8. [PubMed: 3774826]

[88]. Sessler FM, Hsu FC, Felder TN, et al. , Effects of ethanol on rat somatosensory cortical neurons, Brain Res. 804 (2) (1998) 266–274, doi: 10.1016/s0006-8993(98)00680-5. [PubMed: 9757061]

[89]. Zhang WT, Chao THH, Yang Y, et al. , Spectral fiber photometry derives hemoglobin concentration changes for accurate measurement of fluorescent sensor activity, Cell Rep. Methods 2 (7) (2022) 100243, doi: 10.1016/j.crmeth.2022.100243.

[90]. Je HD, Kim HD, Park JH, Controversial effect of ethanol irrespective of kinases inhibition on the agonist-dependant vasoconstriction, Biomol. Ther. 20 (3) (2012) 352–356 (Seoul), doi: 10.4062/biomolther.2012.20.3.352.

[91]. Howes LG, Reid JL, The effects of alcohol on local, neural and humoral cardiovascular regulation, Clin. Sci. 71 (1) (1986) 9–15, doi: 10.1042/cs0710009.

[92]. Kawano Y, Physio-pathological effects of alcohol on the cardiovascular system: its role in hypertension and cardiovascular disease, Hypertens. Res. 33 (3) (2010) 181–191, doi: 10.1038/hr.2009.226. [PubMed: 20075936]

[93]. Drew PJ, Vascular and neural basis of the BOLD signal, Curr. Opin. Neurobiol. 58 (2019) 61–69, doi: 10.1016/j.conb.2019.06.004. [PubMed: 31336326]

[94]. Volkow ND, Hitzemann R, Wolf AP, et al. , Acute effects of ethanol on regional brain glucose metabolism and transport, Psychiatry Res. 35 (1) (1990) 39–48, doi: 10.1016/0925-4927(90)90007-s. [PubMed: 2164230]

[95]. de Wit H, Metz J, Wagner N, Cooper M, Behavioral and subjective effects of ethanol: relationship to cerebral metabolism using PET, Alcohol Clin. Exp. Res. 14 (3) (1990) 482–489, doi: 10.1111/j.1530-0277.1990.tb00508.x. [PubMed: 2198826]

[96]. Volkow ND, Wang GJ, Shokri Kojori E, Fowler JS, Benveniste H, Tomasi D, Alcohol decreases baseline brain glucose metabolism more in heavy drinkers than controls but has no effect on stimulation-induced metabolic increases, J. Neurosci. 35 (7) (2015) 3248–3255, doi: 10.1523/JNEUROSCI.4877-14.2015. [PubMed: 25698759]

[97]. Wilson DF, Matschinsky FM, Ethanol metabolism: the good, the bad, and the ugly, Med. Hypotheses 140 (2020) 109638, doi: 10.1016/j.mehy.2020.109638. [PubMed: 32113062]

[98]. Carboni S, Isola R, Gessa GL, Rossetti ZL, Ethanol prevents the glutamate release induced by N-methyl-D-aspartate in the rat striatum, Neurosci. Lett. 152 (1-2) (1993) 133–136, doi: 10.1016/0304-3940(93)90501-b. [PubMed: 8100051]

[99]. Carton L, Auger F, Kyheng M, et al. , Dose-dependent metabolite changes after ethanol intoxication in rat prefrontal cortex using in vivo magnetic resonance spectroscopy, Sci. Rep. 9 (1) (2019) 10682, doi: 10.1038/s41598-019-47187-4. [PubMed: 31337845]

[100]. Cerri DH, Albaugh DL, Walton LR, et al. , Distinct neurochemical influences on fMRI response polarity in the striatum, BioRxiv (2023) Published online February 21, doi: 10.1101/2023.02.20.529283.

[101]. Katz BM, Walton LR, Houston KM, Cerri DH, Shih YYI, Putative neurochemical and cell type contributions to hemodynamic activity in the rodent caudate putamen, J Cereb. Blood Flow Metab. 43 (4) (2023) 481–498, doi: 10.1177/0271678x221142533. [PubMed: 36448509]

[102]. Dao NC, Brockway DF, Suresh Nair M, Sicher AR, Crowley NA, Somatostatin neurons control an alcohol binge drinking prelimbic microcircuit in mice, Neuropsychopharmacology 46 (11) (2021) 1906–1917, doi: 10.1038/s41386-021-01050-1. [PubMed: 34112959]

[103]. Davies M, The role of GABAA receptors in mediating the effects of alcohol in the central nervous system, J. Psychiatry Neurosci. 28 (4) (2003) 263–274. [PubMed: 12921221]

[104]. Carta M, Ariwodola OJ, Weiner JL, CF. Valenzuela, Alcohol potently inhibits the kainate receptor-dependent excitatory drive of hippocampal interneurons, Proc. Natl. Acad. Sci. U. S. A. 100 (11) (2003) 6813–6818, doi: 10.1073/pnas.1137276100. [PubMed: 12732711]

[105]. Micheva KD, Beaulieu C, Postnatal development of GABA neurons in the rat somatosensory barrel cortex: a quantitative study, Eur. J. Neurosci. 7 (3) (1995) 419–430. [PubMed: 7773439]

[106]. Micheva KD, Beaulieu C, Quantitative aspects of synaptogenesis in the rat barrel field cortex with special reference to GABA circuitry, J. Comput. Neurol. 373 (3) (1996) 340–354 doi: 10.1002/(SICI)1096-9861(19960923)373:3<340::AID-CNE3>3.0.CO;2-2.

[107]. Minelli A, Alonso-Nanclares L, Edwards RH, DeFelipe J, Conti F, Postnatal development of the vesicular GABA transporter in rat cerebral cortex, Neuroscience 117 (2) (2003) 337–346, doi: 10.1016/s0306-4522(02)00864-3. [PubMed: 12614674]

[108]. Walton LR, Verber M, Lee S-H, Chao T-HH, Wightman RM, Shih YYI, Simultaneous fMRI and fast-scan cyclic voltammetry bridges evoked oxygen and neurotransmitter dynamics across spatiotemporal scales, NeuroImage 244 (2021) 118634, doi: 10.1016/j.neuroimage.2021.118634. [PubMed: 34624504]

[109]. Tu W, Zhang N, Neural underpinning of a respiration-associated resting-state fMRI network, eLife 11 (2022), doi: 10.7554/eLife.81555.

[110]. Thompson GJ, J Pan W, SD. Keilholz, Different dynamic resting state fMRI patterns are linked to different frequencies of neural activity, J. Neurophysiol. 114 (1) (2015) 114–124, doi: 10.1152/jn.00235.2015. [PubMed: 26041826]

[111]. Ma Z, Zhang Q, Tu W, Zhang N, Gaining insight into the neural basis of resting-state fMRI signal, NeuroImage 250 (2022) 118960, doi: 10.1016/j.neuroimage.2022.118960. [PubMed: 35121182]

[112]. Liang Z, Ma Y, Watson GDR, Zhang N, Simultaneous GCaMP6-based fiber photometry and fMRI in rats, J. Neurosci. Methods 289 (2017) 31–38, doi: 10.1016/j.jneumeth.2017.07.002. [PubMed: 28687521]

[113]. Chao THH, T Zhang W, Hsu LM, Cerri DH, W Wang T, Shih YYI, Computing hemodynamic response functions from concurrent spectral fiber-photometry and fMRI data, Neurophotonics 9 (3) (2022) 032205, doi: 10.1117/1.NPh.9.3.032205.

[114]. Grandjean J, Desrosiers-Gregoire G, Anckaerts C, et al. , A consensus protocol for functional connectivity analysis in the rat brain, Nat. Neurosci. (2023) Published online March 27, doi: 10.1038/s41593-023-01286-8.

[115]. Harris RA, Trudell JR, Mihic SJ, Ethanol's molecular targets, Sci. Signal 1 (28) (2008) re7, doi: 10.1126/scisignal.128re7.

[116]. Zeller A, Jurd R, Lambert S, et al. , Inhibitory ligand-gated ion channels as substrates for general anesthetic actions, Handb. Exp. Pharmacol. (182) (2008) 31–51, doi: 10.1007/978-3-540-74806-9_2. [PubMed: 18175085]

[117]. Paasonen J, Stenroos P, Laakso H, et al. , Whole-brain studies of spontaneous behavior in head-fixed rats enabled by zero echo time MB-SWIFT fMRI, NeuroImage 250 (2022) 118924, doi: 10.1016/j.neuroimage.2022.118924. [PubMed: 35065267]

[118]. R Gao Y, Ma Y, Zhang Q, et al. , Time to wake up: Studying neurovascular coupling and brain-wide circuit function in the un-anesthetized animal, NeuroImage 153 (2017) 382–398, doi: 10.1016/j.neuroimage.2016.11.069. [PubMed: 27908788]

[119]. Gutierrez-Barragan D, Singh NA, Alvino FG, et al. , Unique spatiotemporal fMRI dynamics in the awake mouse brain, Curr. Biol. 32 (3) (2022) 631–644 e6, doi: 10.1016/j.cub.2021.12.015. [PubMed: 34998465]

[120]. Han Z, Chen W, Chen X, et al. , Awake and behaving mouse fMRI during Go/No-Go task, NeuroImage 188 (2019) 733–742, doi: 10.1016/j.neuroimage.2019.01.002. [PubMed: 30611875]

[121]. MacKinnon MJ, Song S, Ma Y, et al. , Zero-echo-time functional magnetic resonance imaging, J. Cereb. Blood Flow Metab. 42 (2022) 102–103.

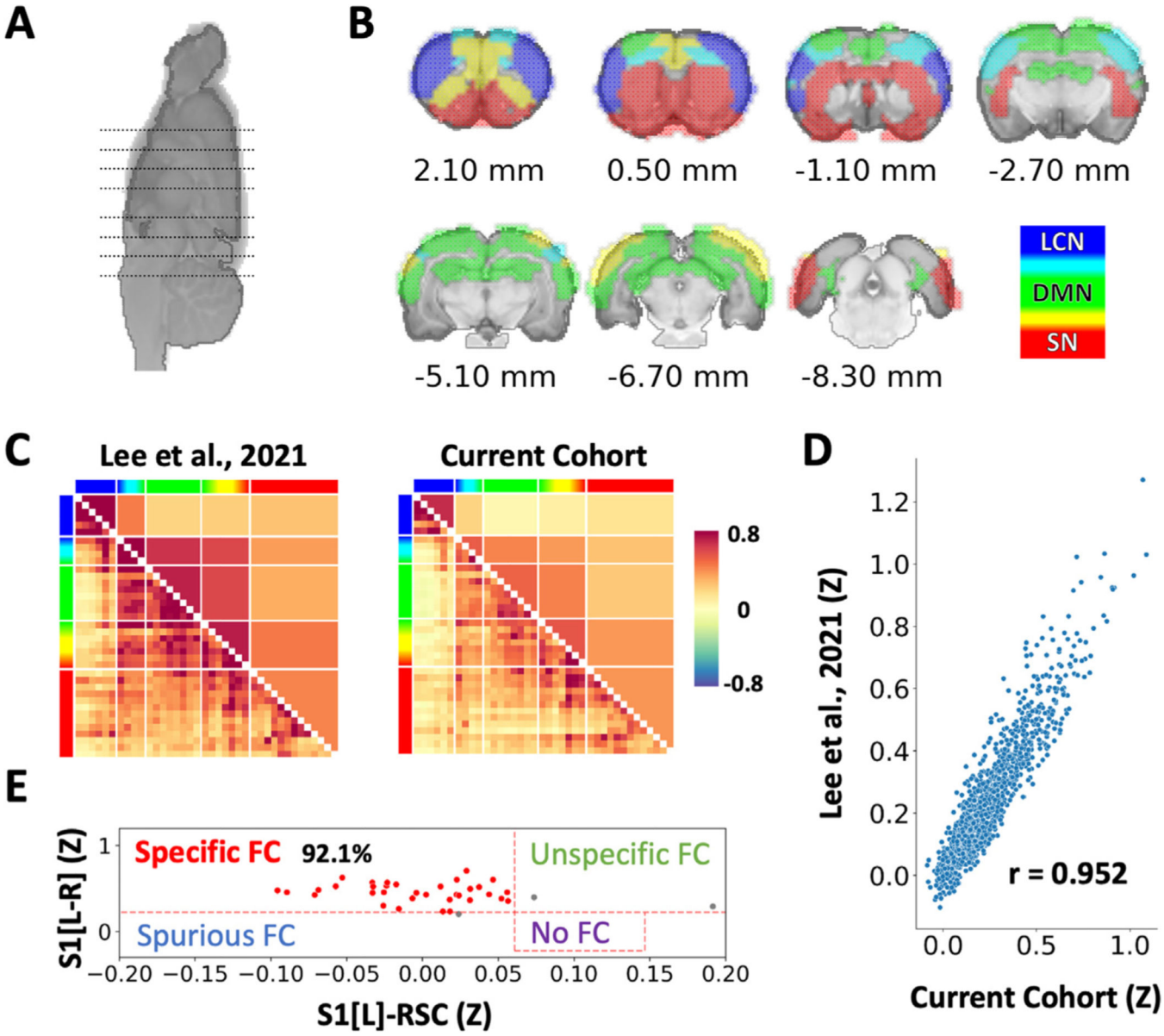

Fig. 1.

Triple networks of the rat brain and reproducibility of functional connectivity measures. (A, B) Triple networks are color-coded and mapped on coronal brain slices with locations indicated in (A). Lateral cortical network (LCN): blue; Default mode network (DMN): green; Salience network (SN): red. The mixed colors between networks indicate network overlaps based on data-driven analysis by [27] and agree with [28]. (C) Comparison of functional connectivity patterns between cohorts. Left: 87 subjects reported in [27] : right: the baseline of current cohort of 38 subjects prior to alcohol administration. Color-bar indicates Fisher's Z score. (D) High spatial correlation of functional connectivity patterns between two cohorts. (E) Functional connectivity specificity analysis supports the quality of the current dataset.

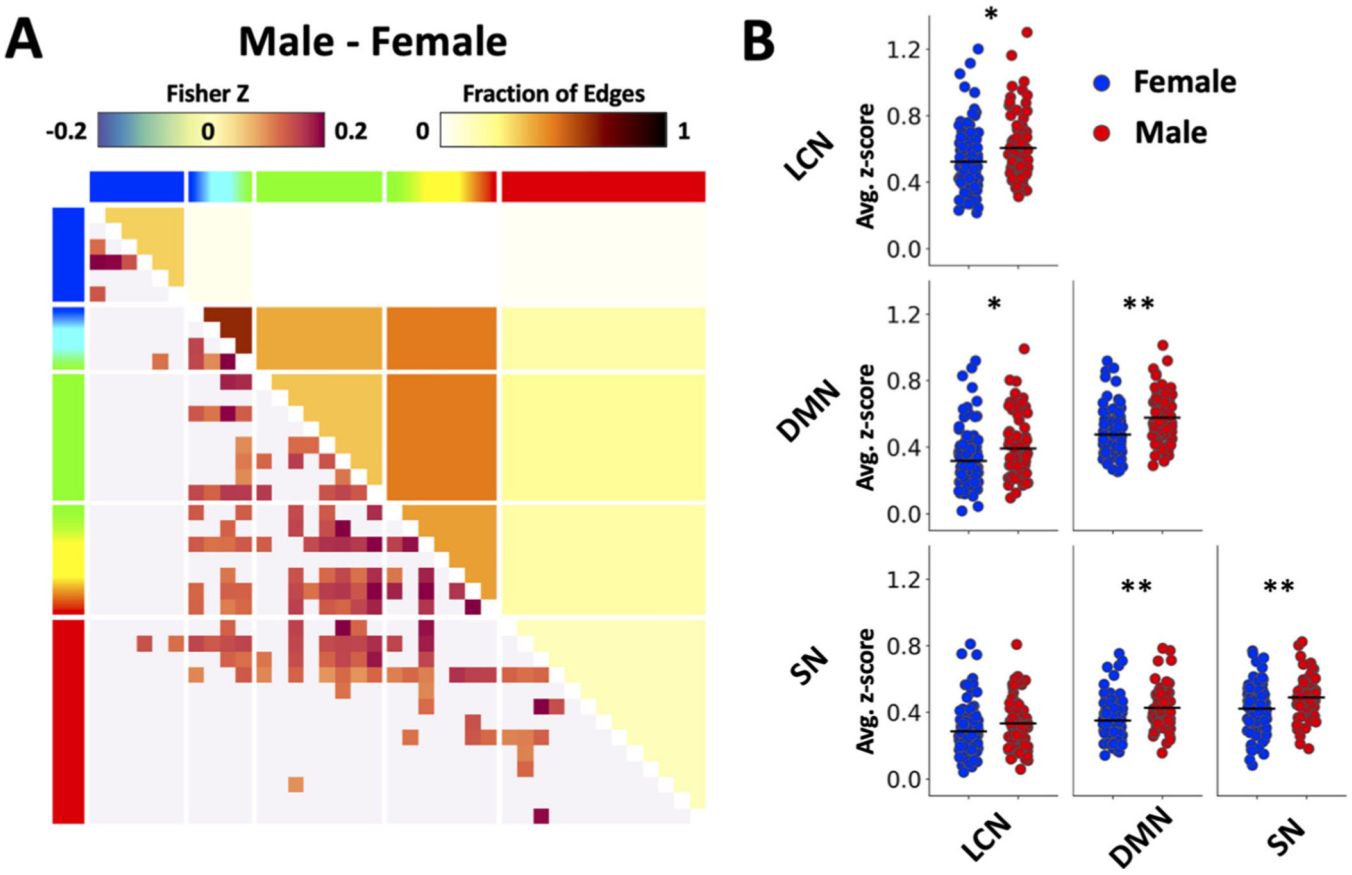

Fig. 2.

Sex effect on functional connectivity. (A) Main effect of sex on connectivity revealed by the GLM analysis. Note that the matrix shows significant differences in overall FC (collapsed across age, baseline and ethanol dosing) between male and female subjects. Functional connectivity (lower left) and fraction of significant edges (upper right) highlight statistically significant differences between sexes ($p < 0.05$). (B) Scatter plots showing sex differences in triple network functional connectivity. Results were generated using the baseline-only data recorded before alcohol injection. Functional connectivity values were averaged across regions within a specific network (* $p < 0.05$, ** $p < 0.01$).

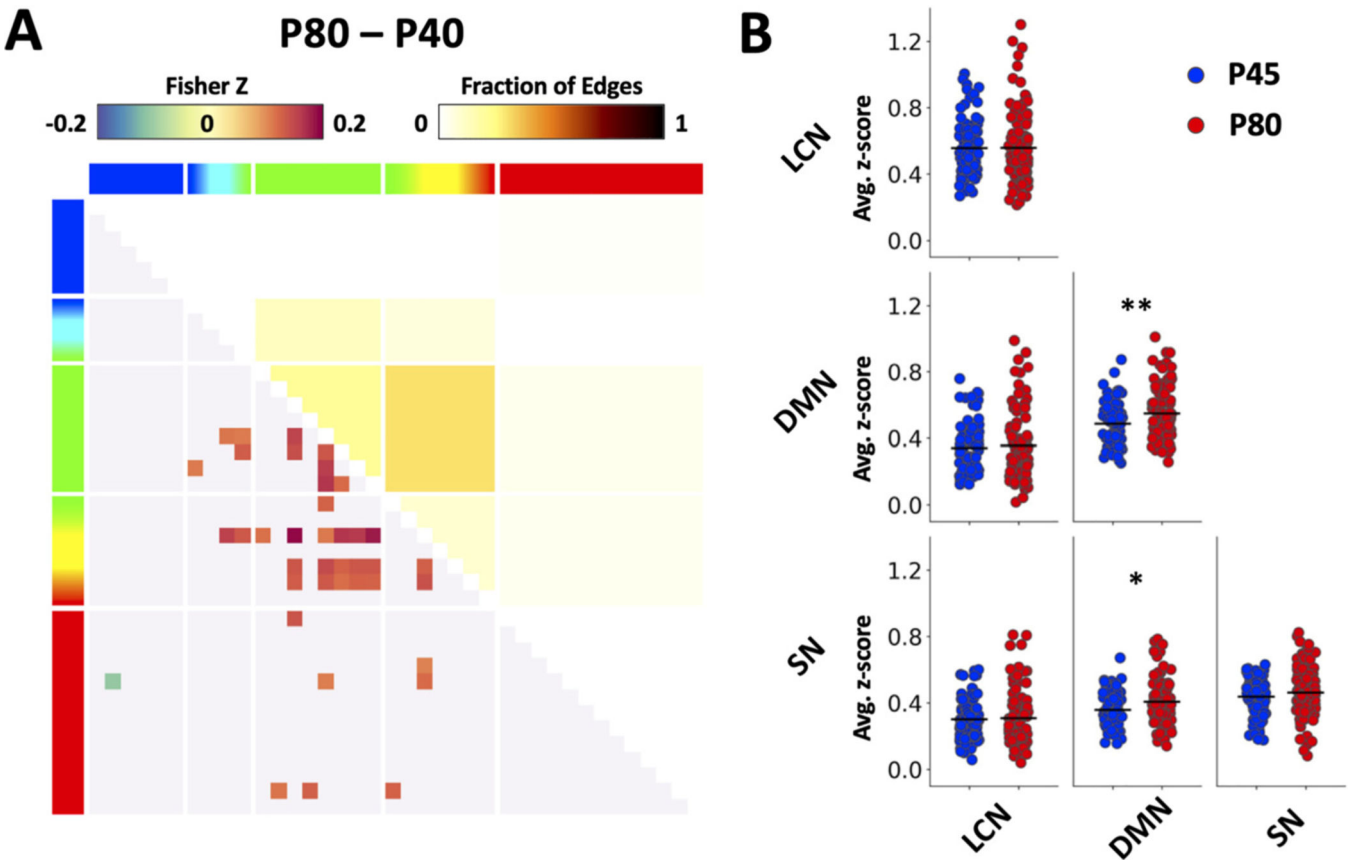

Fig. 3.

Age effect on functional connectivity. (A) Significant main effect of age from GLM analysis. Note that the matrix shows significant differences in overall FC (collapsed across age, baseline and ethanol dosing) between two age-groups. Functional connectivity (lower left) and fraction of significant edges (upper right) highlight statistically significant differences between ages ($p < 0.05$). (B) Scatter plots showing age differences in triple network functional connectivity. Data were generated using the baseline period before alcohol injection. Functional connectivity values were averaged across regions within a specific network (* $p < 0.05$, ** $p < 0.01$).

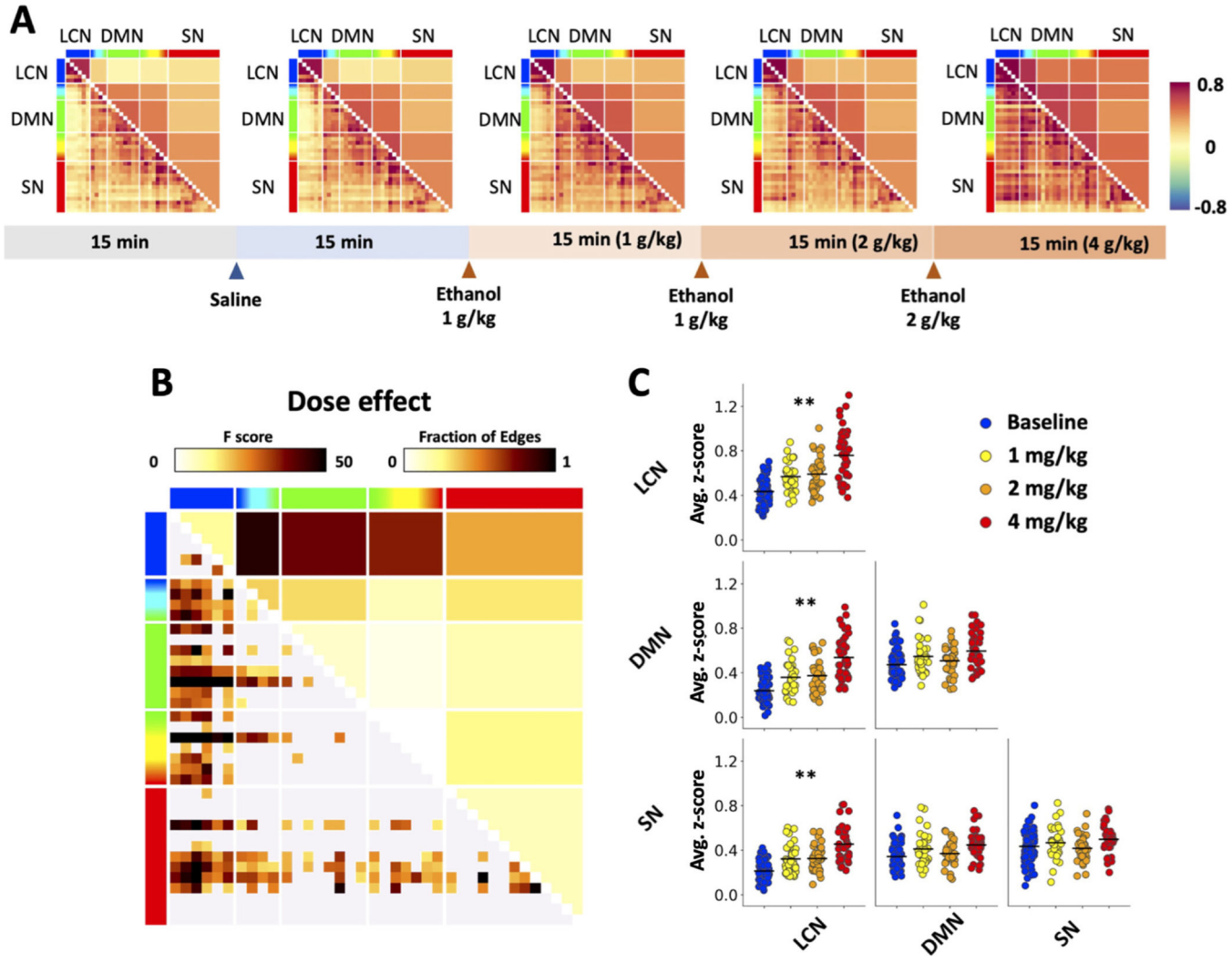

Fig. 4.

Experimental paradigm and population-level functional connectivity changes. (A) An overall increase in functional connectivity was observed after cumulative injections of ethanol. The horizontal bar on the bottom shows the protocol of ethanol dosing. The colorbar on the right indicates Fisher's Z score. (B) Main effect of alcohol dose from GLM. Significant dose-dependent change in functional connectivity (lower left, expressed in F-score) and fraction of significant edges (upper right) highlight statistically significant differences between baseline period and data after ethanol injection ($p < 0.05$). (C) Scatter plots showing ethanol dose-induced functional connectivity differences in triple network functional connectivity. Functional connectivity values were averaged across regions within a specific network (* $p < 0.05$, * * $p < 0.01$).

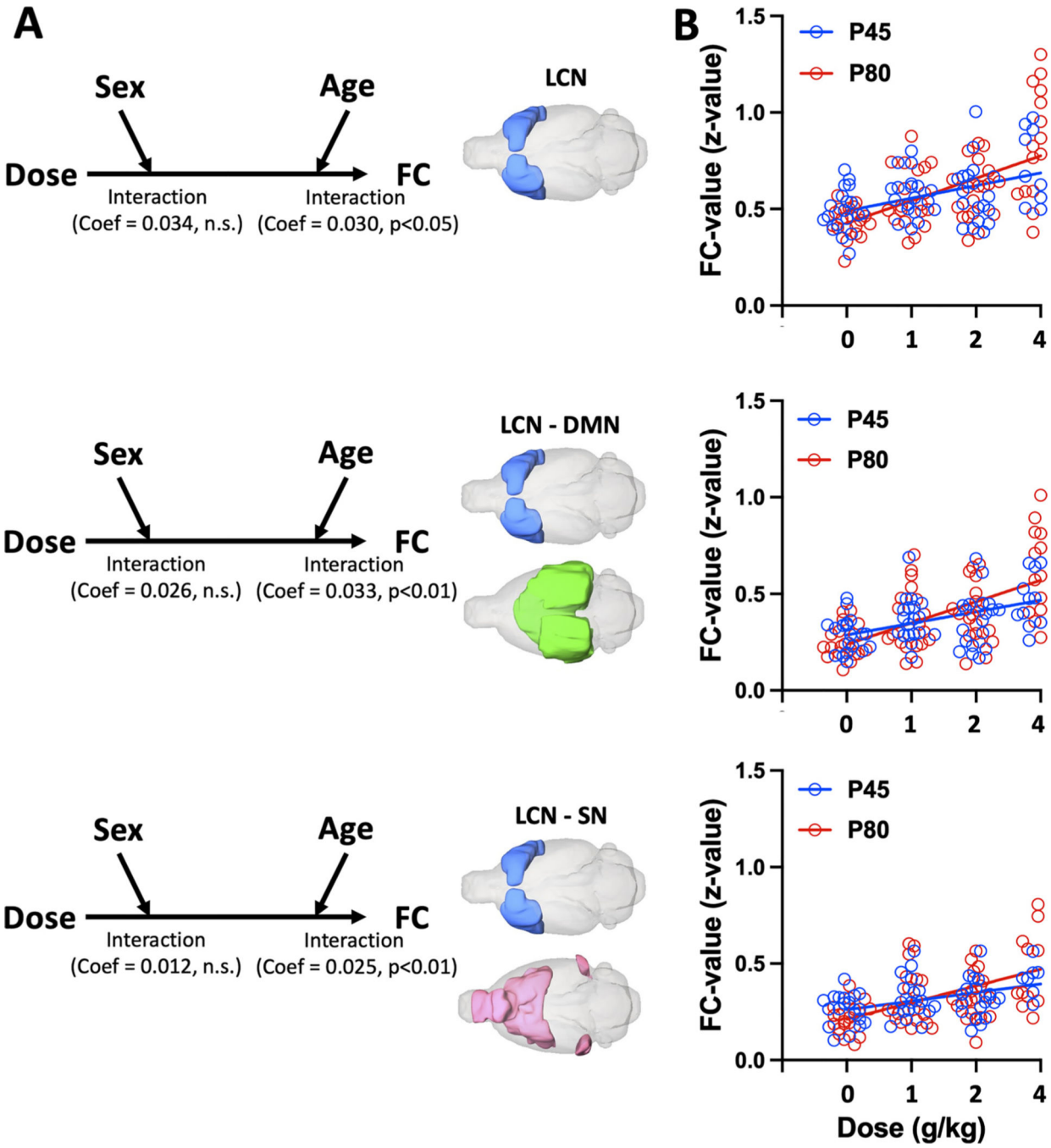

Fig. 5.

Analysis of age effect on the observed EtOH dose-dependent LCN-related FC changes. (A) The three models use EtOH dose, as independent variables, sex and age as moderators, and three network-level FC changes as dependent variables: (top) within LCN, (middle) between LCN and DMN, and (bottom) between LCN and SN. In all three models, main effect of alcohol dose on LCN-related FC was dependent on age (a significant interaction effect, all $p < 0.05$) but not sex (all $p > 0.05$). (B) Dose-dependent increase in LCN-related FC in P45

and P80 groups of rats. Circles indicate data for individual subjects color-coded according to age group. Red and blue lines indicate linear regression slopes.

Table 1

Dose effect estimates from mixed model linear regression analysis.

Age (days)	Network pair	Estimate (z/g/kg)	SE	*P* value	95% CI Lower	Upper
P45	LCN-LCN	0.09	0.013	<0.0001	0.07	0.12
	LCN-DMN	0.08	0.11	<0.0001	0.06	0.1
	LCN-SN	0.06	0.01	<0.0001	0.05	0.08
P80	LCN-LCN	0.15	0.014	<0.0001	0.12	0.17
	LCN-DMN	0.14	0.013	<0.0001	0.11	0.17
	LCN-SN	0.11	0.011	<0.0001	0.09	0.13